

The orbits of the inner Uranian satellites from Hubble Space Telescope and Voyager observations

R.A. Jacobson

Jet Propulsion Laboratory, California Institute of Technology, 4800 Oak Grove Drive, Pasadena, California 91109-8099

Abstract

This article presents revised orbital elements for the ten small Uranian satellites discovered by Voyager 2. The elements have been determined from a fit to astrometric observations made with the Hubble Space Telescope and imaging data acquired by the Voyager 2 spacecraft. An assessment of the accuracy of the orbits represented by the elements is provided as are comparisons with orbits found by previous investigators. Subject headings: planets and satellites: general -- planets and satellites: individual (Uranus) -- solar system: general

1. Introduction

The ten small Uranian satellites were discovered by the Voyager 2 imaging science team (Smith *et al.* 1986). Owen and Synnott (1987, Ref. A) determined orbital elements for them from an analysis of the imaging data. In 1994 the eight outermost of the ten were observed with the Hubble Space Telescope (11 S²1') (Pascu *et al.* 1995, Pascu *et al.* 1996). A subsequent analysis (Pascu *et al.* 1997, Ref. B) produced corrected mean motions for the eight. The purpose of this work is to revise the complete set of orbital elements from a combined analysis of the HST and Voyager observations.

2. Orbit analysis

The Voyager observations are the pixel and line locations of images of the satellites and background reference stars in the Voyager camera frame. The star positions relate the camera pointing and hence the satellite observations to an inertial frame. Owen and Synnott did their analysis in the FK4/B1950 frame taking the star positions from a special star catalogue (Klemola and Owen 1985). To support the work for this paper, we transformed the star positions to the FK5/J2000 system (Yallop *et al.* 1989).

The HST observations are in the form of position angle and separation distance relative to Miranda. In

their reduction Miranda's orbit was represented by the GUST86 analytical theory (Laskar and Jacobson 1987). Comparisons of Miranda-Ariel images with positions predicted from that same theory provided the calibrations for the orientation and scale of the observations.

The analytical model for the inner satellite orbital motion is identical to that of Ref. A, namely, a precessing ellipse referred to the Uranian equator. Six elements and three rates (sidereal mean motion, apsidal secular rate, and nodal secular rate) represent each orbit. The direction of the Uranus spin axis rather than the IAU pole defines the equator. The spin axis orientation is specified by its right ascension, $\alpha(J2000) = 77^{\circ}31127$, and declination, $\delta(J2000) = 15^{\circ}17520$, which are the angles recently determined by French (1997), $\alpha(1950.0) = 76^{\circ}59719$, and declination, $\delta(1950.0) = 15^{\circ}1236$, rotated to the J2000 system following the IAU Commission 20 conversion procedure (Standish *et al.* 1992).

To determine the orbits, we processed the Voyager imaging data set together with the HST observations, correcting the elements and rates for all ten satellites. We estimated five of the elements and the mean motion and used an analytical model (Null *et al.* 1981) to compute the semimajor axis and the apsidal and nodal secular rates. In the semimajor axis and rate computation, the Uranus and satellite masses are from Jacobson *et al.* (1992), and the Uranus gravity zonal harmonics are from French *et al.* (1988). When processing the Voyager optical observations, we took the spacecraft position from the reconstructed Voyager trajectory (Jacobson 1991) rotated to the J2000 system following the IAU Commission 20 conversion procedure.

For the HST data, we assigned a weight corresponding to a 1- σ accuracy of 16 milliarcseconds (mas). This weight is based on the examination of the residuals from a number of trial solutions which used differing weighting schemes. The position angle weight actually applies to the angle scaled by its associated separation distance. This means, for example, that at a separation of 16 seconds of arc, the 1- σ accuracy of the position angle is 1 milliradian. Only observations having residuals less than 48 mas were included in the processing. We set the Voyager data weights at 2.5 times the values used in Ref. A, i.e. weights corresponding to 1- σ accuracies ranging from 0.2 to 0.8 pixel. The original Voyager data weights were conservative; the larger weights provide a better

Table 1: Planetocentric orbital elements referred to the Uranus equator. The epoch is Julian Ephemeris Date 2446450.0 (1986 Jan. 19.5). Longitudes are measured from the node ($90^\circ + \alpha$) of the Uranus equator on the J2000 Earth mean equator. The units are kilometers, degrees, degrees/day, and seconds.

Element	Cordelia (706)	Ophelia (707)	Bianca (708)	Cressida (709)	Desdemona (710)
a	49751.722	53763.390	59165.550	61766730	62658.364
e	0.00026	0.00992	0.00092	0.00036	0.00013
I	0.08479	0.10362	0.19308	0.00568	0.11252
λ	70.00654	298.06836	239.99911	17.43441	314.00041
ϖ	175.20142	181.80964	101.51355	143.63916	129.37318
Ω	38.37431	164.04843	93.22044	99.40335	306.08855
$d\lambda/dt$	1074.518316	956.428333	828.387961	776.582414	760.055539
$d\varpi/dt$	1.502804	1.145001	0.818312	0.703820	0.669358
$d\Omega/dt$	-1.500712	-1.143640	-0.817520	-0.703184	-0.668774
Period	28946.9240	32520.9939	37547.6244	40052.4135	40923.3252
Element	Juliet (711)	Portia (712)	Rosalind (713)	Belinda (714)	Puck (715)
a	64358.222	66097.265	69926.795	75255.613	86004.444
e	0.00066	0.00005	0.00011	0.00007	0.00012
I	0.06546	0.05908	0.27876	0.03063	0.31921
λ	308.67036	340.81170	289.50394	318.96757	331.62360
w	63.97441	122.49946	153.32330	321.74359	85.82748
Ω	200.15504	260.06680	12.84674	279.33720	268.73361
$d\lambda/dt$	730.126135	701.486481	644.630418	577.360289	472.544588
$d\varpi/dt$	0.609477	0.555174	0.455889	0.352762	0.221675
$d\Omega/dt$	-0.608971	-0.554737	-0.455584	-0.352548	-0.221582
Period	42600.8583	44340.1275	48250.9033	53872.7734	65822.3600

measure of the quality of the Voyager data relative to the HST data.

Table 1 gives the new elements and rates. Figures 1 and 2 display the HST observation residuals with the position angle residuals scaled by the separation distance. The three distinct sets apparent in the figures correspond to three different HST orbits. Table 2 gives the statistics of the residuals grouped by satellite. It indicates the number of observations, the sample mean (μ) of the residuals, and the standard deviation (σ) about the mean. The root-mean-square (rms) in the last column is for the total set of observations of the particular satellite and is provided for comparison to the analogous rms given in Ref. B. The statistics show that our orbits fit the HST observations as well, and in some cases better, than Owen

and Synnott's orbits with the revised mean motions of Pascu et al.. Clearly, there is an advantage in correcting all of the orbital elements. The statistics for the complete observation set, which appear as the last entry in the table, verify that the fit is consistent with our data weights. The residuals for the Voyager optical data appear in Figs. 3 and 4; the associated statistics can be found in Table 3. Comparing the pixel and line rms with values from Table II of Ref. A confirms that our orbits fit the optical observations as well as Owen and Synnott's orbits (our Ophelia orbit exhibits asornewhat poorer fit, but the differences are within the data weights).

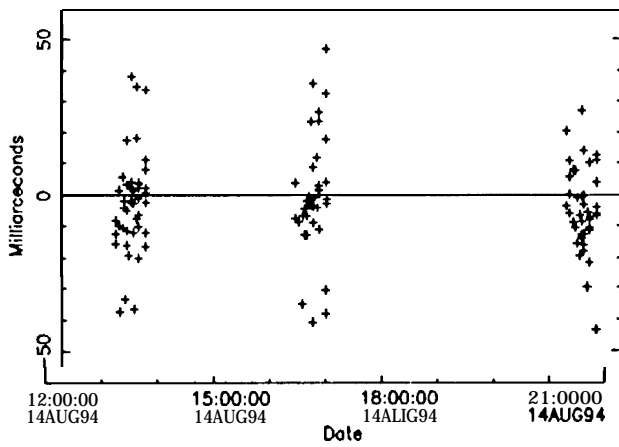


Fig. 1--- HST scaled position angle residuals

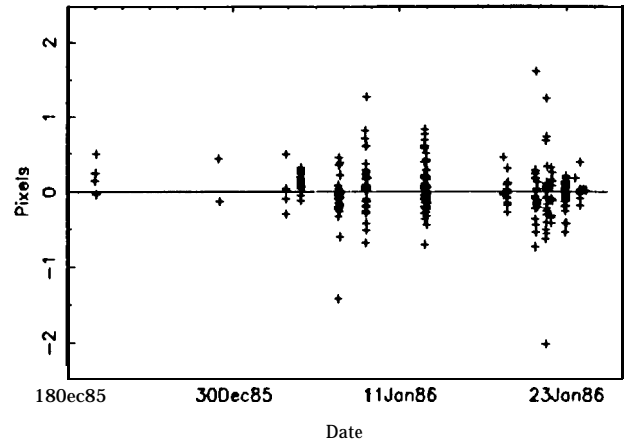


Fig. 3--- Voyager pixel residuals

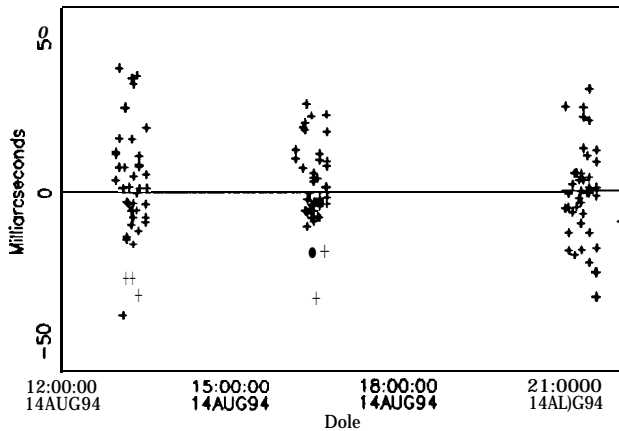


Fig.2--- 11ST separation distance residuals

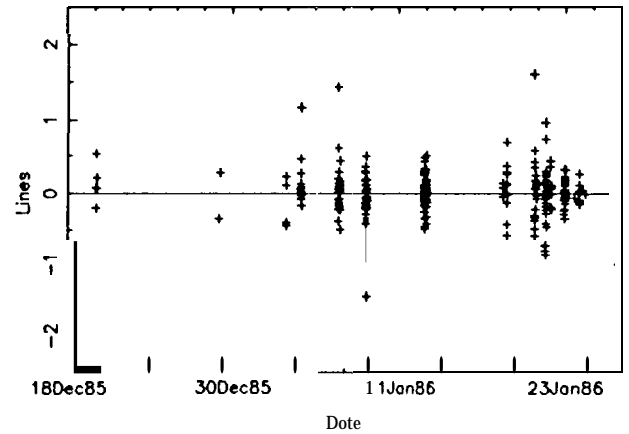


Fig.4--- Voyager line residuals

Table 2: HST Observation Residuals by Satellite. The units are milliarcseconds.

Satellite	Pos. angle			Sep.			rms
	No.	μ	σ	No.	μ	σ	
Bianca	3	35	12	3	4	19	28
Cressida	10	2	8	10	8	16	14
Desdemona	11	-14	20	11	3	20	22
Juliet	17	0	20	17	-1	20	19
Portia	32	-5	13	32	-1	17	16
Rosalind	9	-13	16	9	1	21	20
Belinda	11	8	10	12	-3	16	14
Puck	31	-4	11	32	2	8	10
Total	124	-3	16	126	1	16	16

Table 3: Voyager imaging residual statistics

Object	No.	Pixel			Line		
		μ	σ	rms	μ	σ	rms
Cordelia	24	-0.04	0.67	0.66	0.05	0.41	0.40
Ophelia	13	-0.11	0.21	0.23	0.17	0.45	0.47
Bianca	20	0.04	0.32	0.32	-0.05	0.25	0.25
Cressida	27	0.12	0.42	0.43	-0.07	0.46	0.46
Desdemona	21	-0.02	0.23	0.23	0.02	0.19	0.18
Juliet	38	-0.03	0.16	0.16	0.04	0.22	0.22
Portia	36	-0.03	0.28	0.28	0.07	0.32	0.32
Rosalind	20	0.00	0.28	0.27	-0.04	0.33	0.32
Belinda	35	0.00	0.33	0.32	0.04	0.25	0.25
Puck	49	0.02	0.20	0.19	-0.02	0.19	0.18
Star	796	0.00	0.20	0.20	0.00	0.18	0.18
total	1079	0.00	0.24	0.21	0.00	0.22	0.22

3. Accuracy assessment

The Voyager observations provide accurate measures of the size, shape, and orientation of the orbits. Their highest resolution, 25 km, is about a factor of 6 better than that from HST. Hence, the HST observations add little new information on size, shape, and orientation. However, because the Voyager and HST observations are separated in time by more than 3000 days, together they give a good measure of the mean motions (orbital periods).

Except for the mean motion uncertainties of the eight outermost satellites, the element uncertainties from the combined data fit should be essentially the same as those given in Ref. A. Our element uncertainties, however, are smaller because we used larger weights and did not estimate the semimajor axes as did Owen and Synnott. Table 4 provides the $1-\sigma$ uncertainties for the elements. Comparison of our mean motion statistics with those in Ref. A shows the dramatic improvement due to the HST observations. Our mean motion errors are slightly different from those quoted in Ref. B because of our differing weighting schemes and solution procedure.

The uncertainty in the semimajor axes is dominated by the uncertainty in the GM of Uranus with additional contributions from the uncertainties in the mean motions and Uranus J_2 . Since the publication of Ref. A, there has been nearly a factor of 5 improvement in knowledge of the Uranus GM and an order of magnitude in that of the Uranus J_2 . This improved knowledge together with the reduced mean motion uncertainties leads to significantly smaller semimajor axis statistics than those appearing in Ref. A. The apsidal and nodal rate statistics (not given in Ref. A) follow directly from the uncertainties in the mean motions and Uranus J_2 .

The dominant perturbation on all of the orbits is due to the Uranus J_2 ; it is the only perturbation having a contribution of more than 1 km to the calculated semimajor axis. For all three of the calculated parameters, the J_2 effect is more than two orders of magnitude less than the J_2 , and even in the worst case, Puck, the effects of the major satellites are also more than two orders of magnitude less than J_2 . Consequently, we feel confident calculating rather than estimating the values for the semimajor axis and the apsidal and nodal rates. Any modelling errors introduced from the analytical expressions used in the calculations may be presumed to contribute less than

1 km to the overall orbital uncertainties.

Table 5 gives our assessment of the actual $1-\sigma$ orbit uncertainties during the HST observation time period in the radial, downtrack (in-orbit) and normal (out-of-plane) directions. The downtrack uncertainties include the growth from epoch due to the period uncertainties also given in the table. The table values are based on a mapping of the formal statistics together with comparisons between orbits from a number of trial solutions. The 150 km Miranda orbit error, which affects the HST observations, has a small effect on the mean motion determination. This effect is reflected in the downtrack and period uncertainties. Uncertainty in the downtrack will continue to grow for all ten satellites while, except for Ophelia, the uncertainties in the other directions will remain essentially unchanged in the near future. Because of the significant eccentricity of Ophelia's orbit, its period uncertainty also will feed into its radial direction.

4. Comparison with earlier work

Owen and Synnott determined the elements from only the Voyager data and estimated the semimajor axes as part of their data fit. They also calculated semimajor axis values from a simplified analytical expression using the mean motions from the data fit. In our approach we employed a more complete analytical expression for the semimajor axes and calculated rather than estimating their values (the expressions for the apsidal and nodal secular rates were also more complete). This approach reduces the number of parameters to be determined from seven to six per satellite. Moreover, we believe that the dynamical constraint introduced through semimajor axis calculation leads to a more accurate description of the orbits.

Table 6 contains the differences between the values of selected elements from Ref. A and our results (because of the different reference systems, the longitudes cannot be compared directly). For the semimajor axes the differences are from the calculated values appearing in Ref. A. The semimajor axis, apsis rate, and node rate differences reflect our use of the more complete analytical expressions and the more recent values for the Uranus mass and gravity harmonics,

The mean motion differences for Cordelia and Ophelia we discovered are due to calculating rather than estimating the semimajor axes; a test solution in which we estimated the semimajor axes for the two

Table 4: Orbital element standard deviations. The units arc kilometers, degrees, degrees/day, and seconds.

Element	Cordelia	Ophelia	Bianca	Cressida	Desdemona	Juliet	Portia	Rosalind	Belinda	Puck
a	0.149	0.847	0.045	0.046	0.047	0.048	0.050	0.053	0.057	0.064
e (X10 ³)	0.096	0.107	0.118	0.111	0.070	0.087	0.080	0.103	0.073	0.061
I	0.031	0.055	0.054	0.040	0.037	0.040	0.039	0.045	0.028	0.021
λ	0.011	0.027	0.020	0.013	0.011	0.012	0.010	0.012	0.009	0.007
w	15.0	0.5	10.6	15.1	38.2	8.2	136.9	51.6	51.1	29.7
Ω	8.6	37.9	19.4	360.0	20.8	31.3	33.6	8.0	71.6	3.4
$d\lambda/dt$ ($\times 10^3$)	1.874	9.077	0.042	0.022	0.022	0.018	0.012	0.022	0.017	0.009
$d\omega/dt$ ($\times 10^3$)	0.144	0.114	0.078	0.067	0.064	0.058	0.053	0.044	0.034	0.021
$d\Omega/dt$ ($\times 10^3$)	0.144	0.114	0.078	0.067	0.064	0.058	0.053	0.044	0.034	0.021
Period	0.0505	0.3087	0.0019	0.0011	0.0012	0.0010	0.0008	0.0016	0.0015	0.0012

Table 5: 1- σ Actual orbit uncertainties. The units are kilometers and seconds.

Satellite	Radial	Down track	Normal	Period
Cordelia	50	14500	200	0.15
Ophelia	500	75000	250	0.9
Bianca	30	410	230	0.0060
Cressida	25	220	150	0.0035
Desdemona	25	220	150	0.0035
Juliet	20	185	150	0.0030
Portia	25	175	150	0.0030
Rosalind	25	260	180	0.0050
Belinda	20	220	150	0.0050
Puck	20	200	120	0.0050

satellites leads to the same mean motions as those in Ref. A. The differences between our values for eccentricity and inclination and the Ref. A values also stem from our use of the calculated semimajor axes. The inclination differences contain a small additional contribution due to the revised Uranus equator orientation. For the eight satellites observed with HST the element changes are a consequence of processing those observations coupled with a secondary contribution from the use of the calculated semimajor axes.

Table 6 also gives the differences between our mean motions and those quoted in Ref. R. For seven of the satellites the differences are near or below the level of the combined uncertainty (root-sum-square of our uncertainty and that of Ref. B). For Puck, however, the difference is about 2.5 times the combined uncertainty. In an effort to understand the mean motion disagreement, we repeated the analysis of Ref. B, i.e., corrected only the mean motions based on the HST

observations. Differences between ‘these mean motions and those from Ref. B appear as the last entry in Table 6; the differences nearly match the ones associated with our mean motions determined with the combination of Voyager and HST data. We conjecture that the source of the mean motion disagreement is some slight difference between our method and that used by the Ref. B authors to compute the HST observables; we are getting nearly the same residuals with slightly different orbits. The formal statistics do not reflect small variations in computational procedures. We have, however, attempted to account for such variations as well as for other unmodelled effects in our actual uncertainties in Table 5.

Another form of orbit comparison appears in Table 7 where differences are provided in terms of cylindrical coordinates referred to the Uranus equator. The angle in the Uranus equator is the angular separation on 14 August 1994 and primarily reflects the effects of the different mean motions. Angles are given for the mean motions of both Ref. A and Ref. R. The columns labeled ‘R’ and ‘Z’ contain the absolute values of the maximum difference in those components within the time period 13 August 1994 to 15 August 1994. The radial component is directly affected by changes in semimajor axis, eccentricity, longitude of periapsis, and mean longitude. The normal component is directly affected by changes in inclination, longitude of the ascending node, and mean longitude.

5. Concluding remarks

This article has reported on a new determination of the orbits of the inner Uranian satellites from imaging

Table 6: Orbital element differences. The units are kilometers, degrees, and degrees/day.

Element	Cordelia	Ophelia	Bianca	Cressida	Desdemona	Juliet	Portia	Rosalind	Belinda	Puck
a	-0.022	0.910	-0.150	0.070	0.136	0.078	0.035	0.005	-0.213	-0.044
$e(\times 10^3)$	0.207	0.218	-0.037	-0.128	0.101	-0.075	0.113	-0.023	0.036	-0.067
I	0.055	-0.013	-0.037	0.037	0.048	-0.008	0.027	0.003	0.002	-0.005
$d\omega/dt(\times 10^3)$	4.863	3.177	1.849	1.361	1.212	0.977	0.755	0.343	-0.114	-0.861
$d\Omega/dt(\times 10^3)$	-4.884	-3.182	-1.846	-1.363	-1.218	-0.978	-0.757	-0.344	0.114	0.862
$d\lambda/dt(\times 10^3)$	2.257	-21.518	3.516	-0.783	-2.370	-0.769	0.106	0.708	2.529	0.482
$d\lambda/dt(\times 10^3)$ Ref. B			-0.013	0.033	-0.021	-0.006	-0.013	0.012	0.019	-0.032
$d\lambda/dt(\times 10^3)$ HST only minus Ref. B			-0.012	0.031	-0.013	-0.008	-0.013	0.014	0.020	-0.029

observations obtained by the Voyager 2 spacecraft and observations acquired with the Hubble Space Telescope. The revised elements are referred to the equator of Uranus as defined by a revised spin axis. All work was done in the J2000 rather than B1950 system, and the latest set of masses and Uranus gravity harmonics were used in the calculation of the semimajor axes, apsidal rates, and nodal rates. The article has also included an assessment of the accuracy of the orbits and a comparison with previously published orbits.

Table 7: Uranian equatorial system differences at the time of the 11ST observations. R is distance (km) from the pole, T is angle(deg) in the equator, Z is distance (km) normal to the equator.

Satellite	R	T(A)	T(B)	Z
Cordelia	39	7.016		110
Ophelia	687	-66.003		178
Bianca	10	11.002	-0.019	98
Cressida	20	-2.433	0.117	52
Desdemona	24	-7.395	-0.042	67
Juliet	14	-2.403	-0.019	19
Portia	19	0.316	-0.057	52
Rosalind	22	2.223	0.045	59
Belinda	3	7.919	0.068	28
Puck	16	1.512	-0.094	20

Because of the HST observations, knowledge of the orbits of eight of the ten satellites has significantly improved. Predictions based on our updated orbits of those eight should be sufficiently accurate to support observations for the near future. New observations

of Cordelia and Ophelia are needed to bring knowledge of their periods to the level of that of the other satellites.

Ephemerides based on the orbits in this article are available electronically from the JPL Horizons on-line solar system data and ephemeris computation service (Giorgini *et al.* 1996).

The author wishes to thank D. Pascu and his co-authors for the prepublication copy of the article on the HST observations and for valuable discussions concerning them. The author also wishes to thank W. Owen for his assistance with the Voyager observations and for access to his records of the analysis done for Ref. A. The research described in this publication was carried out by the Jet Propulsion Laboratory, California Institute of Technology, under a contract with the National Aeronautics and Space Administration.

REFERENCES

- French, R. G., Elliot, J.I., French, L. M., Kangas, J. A., Meech, K. J., Ressler, M. E., Buie, M. W., Frogel, J. A., Holberg, J.B., Fuensalida, J. J., Joy, M. 1988, *Icarus*, 73, 349
- French, R.G. 1997, Private communication
- Giorgini, J. D., Yeomans, D.K., Chamberlain, A. R., Chodas, P. W., Jacobson, R. A., Keesey, M. S., Lieske, J. H., Ostro, S. J., Standish, E.M., Wimmerly, R.N. 1996, 28th Annual Meeting of the Division for Planetary Sciences of the American Astronomical Society, Tucson, Az
- Jacobson, R.A. 1991, 'Voyager 2 Uranus Reconstruction - Update', JPL IOM 314.6-1377, Jet Propulsion

sion Laboratory, Pasadena, CA (internal document)

Jacobson, R. A., Campbell, J. K., Taylor, A.H., Synnott, S.P. 1992, AJ, 103, 2068

Klemola, A. R., Owen, W.M. 1985, Uranus-Voyager Reference Star Catalogue, Lick Observatory, Santa Cruz, California

Laskar, J., Jacobson, R.A. 1987, A&A, 188, 212

Null, G. W., Lau, E.L., Biller, E. D., Anderson, J.D. 1981, AJ, 86, 456

Owen, W. M., Synnott, S.P. 1987, AJ, 93, 1268 (Ref. A)

Pascu, D., Rohde, J. R., Seidelmann, P. K., Currie, D. G., Dowling, D. M., Wells, E., Kowal, C., Zellner, B., Storrs, A. 1995, BAAS, 186, 1302

Pascu, D., Rohde, J. R., Seidelmann, P. K., Wells, E., Kowal, C., Zellner, B., Storrs, A., Currie, D. G., Dowling, D.M. 1996, BAAS, 28, 1184

Pascu, D., Rohde, J. R., Seidelmann, P. K., Wells, E., Kowal, C., Zellner, B., Storrs, A., Currie, D. G., Dowling, D.M. 1997, submitted to AJ (Ref. B)

Smith, B. A., Soderblom, L. A., Beebe, R., Bliss, D., Boyce, J. M., Brahic, A., Briggs, G. A., Brown, R.H., Collins, A., Cook II, A. F., Croft, S. K., Cuzzi, J. N., Danielson, G. E., Davies, M. E., Dowling, T. E., Godfrey, D., Hansen, C. J., Harris, C., Hunt, G. E., Ingersoll, A. P., Johnson, T. V., Krauss, R. J., Masursky, H., Morrison, D., Owen, T., Plescia, J. B., Pollack, J. B., Porco, C. C., Rages, K., Sagan, C., Shoemaker, E. M., Stromovsky, L. A., Stoker, C., Strom, R. G., Suomi, V. E., Synnott, S.P., Terrile, R. J., Thomas, P., Thompson, W. R., Veverka, J. 1986, Science, 233, 43

Standish, F. M., Newhall, X X, Williams, J. G., Yeomans, D.K. 1992, in Explanatory Supplement to the Astronomical Almanac, P.K. Seidelmann, cd., University Science Books, Mill Valley, CA

Yallop, B. D., Hohenkerk, C. Y., Smith, C. A., Kaplan, G.H., Hughes, J. A., Seidelmann, P.K. 1989, AJ, 97, 274